Azidohomoalanine: A Minimally Invasive, Versatile, and Sensitive Infrared Label in Proteins To Study Ligand Binding

Zanobini, Claudio ; Bozovic, Olga ; Jankovic, Brankica ; Koziol, Klemens L ; Johnson, Philip J M ; Hamm, Peter ; Gulzar, Adnan ; Wolf, Steffen ; Stock, Gerhard

Abstract: The noncanonical amino acid azidohomoalanine (Aha) is known to be an environment-sensitive infrared probe for the site-specific investigation of protein structure and dynamics. Here, the capability of that label is explored to detect protein ligand interactions by incorporating it in the vicinity of the binding groove of a PDZ2 domain. Circular dichroism and isothermal titration calorimetry measurements reveal that the perturbation of the protein system by mutation is negligible, with minimal influence on protein stability and binding affinity. Two-dimensional infrared spectra exhibit small (1-3 cm(-1)) but clearly measurable red shifts of the Aha vibrational frequency upon binding of two different peptide ligands, while accompanying molecular dynamics simulations suggest that these red shifts are induced by polar contacts with side chains of the peptide ligands. Hence, Aha is a versatile and minimally invasive vibrational label that is not only able to report on large structural changes during, e.g., protein folding, but also on very subtle changes of the electrostatic environment upon ligand binding.

DOI: https://doi.org/10.1021/acs.jpcb.8b08368

Azidohomoalanine: A Minimally-Invasive, Versatile and Sensitive Infrared Label in Proteins to Study Ligand Binding

Claudio Zanobini, Olga Bozovic, Brankica Jankovic, Klemens L. Koziol, Philip J. M. Johnson, Peter Hamm*
Department of Chemistry, University of Zurich, Zurich, Switzerland
and
Adnan Gulzar, Steffen Wolf, Gerhard Stock*
Biomolecular Dynamics, Institute of Physics, Albert Ludwigs University, Freiburg, Germany

* *corresponding authors:* peter.hamm@chem.uzh.ch and stock@physik.uni-freiburg.de
(Dated: October 17, 2018)

Abstract: The noncanonical amino acid azidohomoalanine (Aha) is known to be an environment-sensitive infrared probe for the site-specific investigation of protein structure and dynamics. Here, the capability of that label is explored to detect protein-ligand interactions by incorporating it in the vicinity of the binding groove of a PDZ2 domain. Circular dichroism (CD) and isothermal titration calorimetry (ITC) measurements reveal that the perturbation of the protein system by the mutation is negligible, with minimal influence on protein stability and binding affinity. Two dimensional infrared (2D IR) spectra exhibit small (1-3 cm^{-1}) but clearly measurable red shifts of the Aha vibrational frequency upon binding of two different peptide ligands, while accompanying molecular dynamics (MD) simulations suggest that these red shifts are induced by polar contacts with side chains of the peptide ligands. Hence, Aha is a versatile and minimally invasive vibrational label that is not only able to report on large structural changes during e.g. protein folding, but also on very subtle changes of the electrostatic environment upon ligand binding.

I. INTRODUCTION

Proteins are key mediators in virtually every biological process exhibiting their functions through specific interactions with other proteins, peptides, nucleic acids, small molecules, or ions.[1–3] Vital information in the cell is transmitted through specific non-covalent interactions in *e.g.* signal transduction cascades, regulation of metabolic processes, activation or inhibition of enzymatic reactions, assembly of macromolecular complexes, and programmed cell death.[4,5] Disruption of specific interactions is a major cause of numerous diseases. Therefore, understanding structural details of protein-ligand interactions is a prerequisite for clarifying cellular processes at a molecular level.[6] Furthermore, knowledge of the mechanisms of protein-ligand recognition facilitates rational drug design for treatments of different diseases.[7–9] Because of its importance, a plethora of methods for protein-ligand binding analysis have been developed.[10–12]. Specificity is one of the crucial features of protein-ligand interactions and therefore methods that can directly discriminate between specific and non-specific binding are advantageous.[13,14]

It has recently been demonstrated that the presence of an infrared label at the site of recognition between a protein and its binding partner can give site specific insight into the underlying mechanisms of how signaling proteins function.[15–19] Such studies require a special vibrational label that absorbs in the spectral window between ≈1700 cm^{-1} to ≈2800 cm^{-1} in order to discriminate it from a huge protein background.[20–25] Among the possible molecular groups that have been proposed in that regard,[16,17,19,26–44] we favor the noncanonical amino acid azidohomoalanine (Aha). Aha has a relatively high extinction coefficient (≈300-400 $M^{-1}cm^{-1}$),[15] and it has been shown to be an environment-sensitive infrared probe, capable of sensing the polarity of its environment via the frequency of its vibrational transition[15,18,28,45–47] Additionally, this noncanonical amino acid can be incorporated into a protein in virtually any position via methionine-auxotrophic expression strategy.[48–50] All these characteristics make Aha one of the most promising IR labels.

For the most part, Aha has only been used to detect quite significant structural changes in protein structure. For example, unfolding of an Aha mutant has been investigated, where the effect has been the largest when the label is incorporated in the core of the protein, with a frequency blue shift of 19 cm^{-1} upon thermal denaturation.[45] In that case, not only the structure of the protein changes dramatically upon unfolding, but the environment of the Aha label also changes from hydrophobic in the core of a protein to fully solvent exposed. With regard to ligand binding, on the other hand, the Aha label has been incorporated into peptide fragments derived from the Ras-associated guanine nucleotide exchange factor 2 (Ra-GEF2),[15,18] whose C-terminal domain interacts with the PDZ2 domain of human phosphatase 1E.[51] PDZ-domain containing proteins mediate a wide variety of signaling processes in diverse organisms and thus represent excellent model systems for peptide binding studies.[52] Upon binding to a PDZ2 domain, the peptide ligand undergoes a structural change that is comparable to protein folding, that is, the peptide is a solvent-exposed random coil in its unbound state, but structurally well defined in its bound state. Furthermore, depending on the position of the Aha label, it points into the rather hydrophobic binding pocket, and conse-

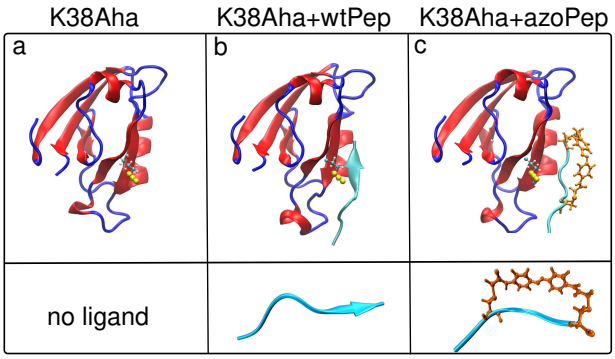

FIG. 1. Molecular systems considered in this study. (a) The K38Aha mutant of apo-PDZ2 with the Aha label indicated in balls and sticks, (b) with the wild-type peptide bound to its binding groove (K38Aha+wtPep), and (c) with azobenzene-variant of the peptide bound to the binding groove (K38Aha+azoPep); azobenzene photoswitch displayed as orange sticks. The shown structures are snapshots taken from the MD simulation.

quently, a frequency shift of similar size (15 cm^{-1}) has been observed.[18]

With the present paper, we set out to explore how far we can push the method. That is, rather than having the Aha label in the peptide ligand,[15,18] we incorporate it in the protein sequence near the binding pocket at position K38. This site was chosen since previous MD simulations have suggested frequent salt-bridges of the peptide ligand with K38 during the process of binding.[53] Hence, we expect at most a marginal structural change of the protein upon ligand binding,[54] but the ligand will still modulate the degree of solvation of the Aha label. We apply 2D IR spectroscopy[55] in a dedicated 2D IR spectrometer[23] in order to be sensitive enough to measure very small frequency shifts of the Aha vibration. For the purpose of this work, the advantage of 2D IR spectroscopy is its quadratic signal dependence on the absorption cross section, which to a significant extent suppresses the strong water background. We furthermore present molecular dynamics (MD) simulations aimed to provide microscopic information on the structural changes around the binding pocket, and the mechanisms of solvation of the Aha label.

We considered the three molecular systems shown in Fig. 1 in this study. As a reference sample, we measured and MD simulated the K38Aha mutant of apo-PDZ2 (denoted K38Aha throughout this paper, see Fig. 1a). We then bound either the wild-type peptide (RWAKSEAKENEQVSAV) to its binding groove (denoted K38Aha+wtPep, see Fig. 1b), or a mutant of that peptide (RWAKSEAKECEQVSCV) with an apolar azobenzene moiety attached to the peptide via the two cysteines (denoted K38Aha+azoPep, see Fig. 1c). The azobenzene variant has originally been developed to photoswitch the binding affinity of the peptide ligand, which will be the topic of another publication. Here, we make use of the hydrophobicity of the azobenzene moiety, which might affect the degree of solvation of the Aha label (note that in contrast to our previous studies,[50,56,57] the azobenzene moiety does not contain any -SO_3^- groups). All experiments have been performed in the dark to ensure that the azobenzene moiety is in its *trans* configuration.

II. METHODS

A. Protein and Peptide Preparation

Expression of the K38Aha mutant of PDZ2 domain was performed as described earlier.[49,50] The two peptide variants, wild type peptide (RWAKSEAKENEQVSAV) and its cysteine mutant ((RWAKSEAKECEQVSCV), were synthesized using solid phase peptide synthesis with standard 9-fluorenylmethoxycarbonyl (Fmoc) chemistry on a Liberty 1 peptide synthesizer (CEM Corporation, Matthews, NC, USA). The crude products were purified using reverse phase HPLC with a C18 column (Macherey Nagel, Dren, Germany), 0.1% TFA buffered acetonitrile gradient 0-50% in 10 column volumes.

The second peptide variant was linked to the azobenzene moiety (diiodoacetamide azobenzene) as reported previously[58] with the following modifications: 50 μmol of peptide was dissolved in 75 mL of 20 mM TRIS buffer, pH 8.5, which was previously extensively degassed. In order to promote the linking reaction by reducing disulphide bridges between cysteines, one equivalent of TCEP was added to peptide solution and allowed to incubate for one hour after which 100 μmol of azobenzene linker dissolved in 250 mL of THF was added. The solution was stirred and left in the dark at room temperature overnight. The linked peptide was concentrated at 30 °C to precipitate the excess of apolar azobenzene linker. The suspension was filtered and the linked azo peptide was repurified using reverse phase HPLC with a C18 column.

All products, protein and both peptides, were dialyzed against 50 mM borate, 150 mM NaCl buffer, pH 8.5, lyophilized, and finally resuspended in H_2O for the circular dichroism (CD) and isothermal titration calorimetry (ITC) measurements and D_2O for the 2D IR measurements. Purity of all samples was confirmed by mass spectrometry analysis.

B. 2D IR Spectroscopy

2D IR spectra in the boxcar geometry were measured using mid-IR pulses generated by a home-built optical parametric amplifier[59] providing ≈150 fs FWHM, ≈2 μJ pulses at ≈5 μm with a repetition rate of 5 kHz, as previously described.[18] A syringe pump sample delivery system was used to flow either sample or buffer through a cell comprised of two CaF_2 windows (2 mm thickness, 25 mm diameter) with a 25 μm teflon spacer. 2D IR spectra of the buffer and of the sample solutions were

measured independently, exchanging approximately 250-300 μL of sample per measurement with the help of the syringe pumps. Buffer and sample spectra were phased individually, using the water background for a reference phase as described previously,[60] and then subtracted to reveal the isolated Aha signal.

C. Computational Methods

The starting structure of PDZ2 was taken from PDB entry 3LNX.[61] To generate initial structures for the MD simulations of K38Aha+wtPep, we extracted the peptide structure and position from the X-ray structure 3LNY,[61] which contains an only 6 residues long peptide ligand, and attached 3 additional residues from the NMR structure of 1D5G[54] at the N-terminus. The peptide considered in the MD simulation (KENEQVSAV) thus is shorter than in experiment. K38 was mutated to Aha in all systems.

The MD equilibrium simulations with a production run length of 100 ns were performed using the GROMACS software package v2016.3[62] with a hybrid GPU-CPU acceleration scheme and the AMBER99SB-*ILDN forcefields as described in ref. 50. Azo-switch parameters were obtained using Antechamber[63] with BCC charges[64,65] and are described in the Supplementary Materials. We used a dodecahedral box with an image (i.e., face-to-face) distance of 7 nm. The box contained 7495 (K38Aha), 7997 (K38Aha+wtPep) and 10168 (K38Aha+azoPep) water molecules, respectively. Further simulation details can be found in Ref. 50.

To determine -N_3 contacts with the protein and the ligand, *g_mindist* from the Gromacs tools was employed. Contact distributions were then obtained by histogramming the MD data with 0.01 nm binning width. We define a contact to be formed if the minimal distance between azido group nitrogen atoms and protein/ligand residue is shorter than 0.45 nm.[66,67] In a similar way, we analyzed contacts between Aha and water as azido group/water oxygen atom distances with a cutoff of 0.45 nm.

We used the empirical model of Cho and co-workers[47] to estimate vibrational frequency shifts $\delta\omega$ caused by changes in the electrostatic environment of the Aha labels. By calculating the electric field $E_j(t)$ at the nitrogen atoms (j = 1, 2, 3) of the azido group for each MD snapshot at time t, we obtain the spectral shift (relative to the vacuum value)

$$\delta\omega(t) = \sum_j a_j E_j(t) \tag{1}$$

with coefficients a_j given in Ref. 47. Electric fields were computed via a reaction field approach using a cutoff radius r_c = 2.3 nm as described in Ref. 50. From the frequency trajectory $\delta\omega(t)$ with a time step of 15 ps, the distribution of the vibrational shifts was obtained via a histogram using 50 bins between -25 and 25 cm^{-1}.

III. RESULTS

A. Experimental Results

To set the stage, we start with verifying that the Aha label only minimally disturbs the protein system. To that end, temperature dependent CD signals were recorded at 205 nm, revealing a melting temperatures of 44 ± 1°C and 46 ± 1°C for wild-type PDZ2 and K38Aha (Fig. S1, Supplementary Material), respectively. Hence, the mutation to Aha in fact slightly stabilizes the protein. Moreover, the dissociation constants of the wild-type peptide to wild-type protein and K38Aha are virtually the same (K_D=11 μM, see Fig. S2a,b, Supplementary Material). This is the evidence of the fact that the energy of binding has not been affected by substituting Aha in the vicinity of the binding groove of the protein. We also measured the binding affinity of the azo-peptide to K38Aha, revealing a somewhat smaller value (K_D=3 μM, see Fig. S2c, Supplementary Material) as compared to the wild-type peptide, indicating that the azo-moiety points away from the binding groove when bound to the protein, but capable of interacting with the protein in a stabilizing manner.

Fig. 2, top panels, show 2D IR spectra of the Aha vibrational label of all three sample systems (we concentrate here on the ground-state (0-1) peak of the 2D IR response on the diagonal, while the excited state (1-2) peak is outside the frequency window shown in Fig. 2). The concentrations used in these experiments were 0.9 mM for the protein, and 2.5 mM and 1.5 mM for wildtype and the azo-peptide, respectively. Given the binding affinities of both peptides in the low μM range (see Supplementary Material, Fig. S2), practically 100% of the protein, which carries the Aha label, has a ligand bound at these concentrations. Fig. 2, bottom panels show diagonal cuts through the 2D-IR spectra (averaging over the diagonal and the two first off-diagonals). To determine the peak frequency of the label, we fit these diagonal cuts to a line-shape function. We found that the quality of the fit is better when using a Lorentzian rather than a Gaussian line-shape, and we added a tilted linear baseline to the fit, which accounts for a residual water background. We considered the center of the fitted Lorentzian to be the peak position of the corresponding peak band. That procedure revealed a peak position of 2113.7 cm^{-1} for K38Aha (marked as dotted vertical lines in Fig. 2 a,b,c), and red shifted peaks at 2112.5 cm^{-1} for K38Aha+wtPep and 2111.0 cm^{-1} for K38Aha+azoPep (solid vertical lines in Fig. 2 b,c). In K38Aha, the linewidth is 20.5 cm^{-1} FWHM together with a rather round 2D IR lineshape (justifying the Lorentzian fit). Upon binding of a ligand, the linewidth increases a little bit (23.6 cm^{-1} for K38Aha+wtPep and 22.6 cm^{-1} for K38Aha+azoPep) and the 2D IR lineshape becomes more elongated along the diagonal, indicating a more inhomogeneously broadened absorption band.

By repeating these experiments various times (i.e., between 2-4 times for different samples), taking into ac-

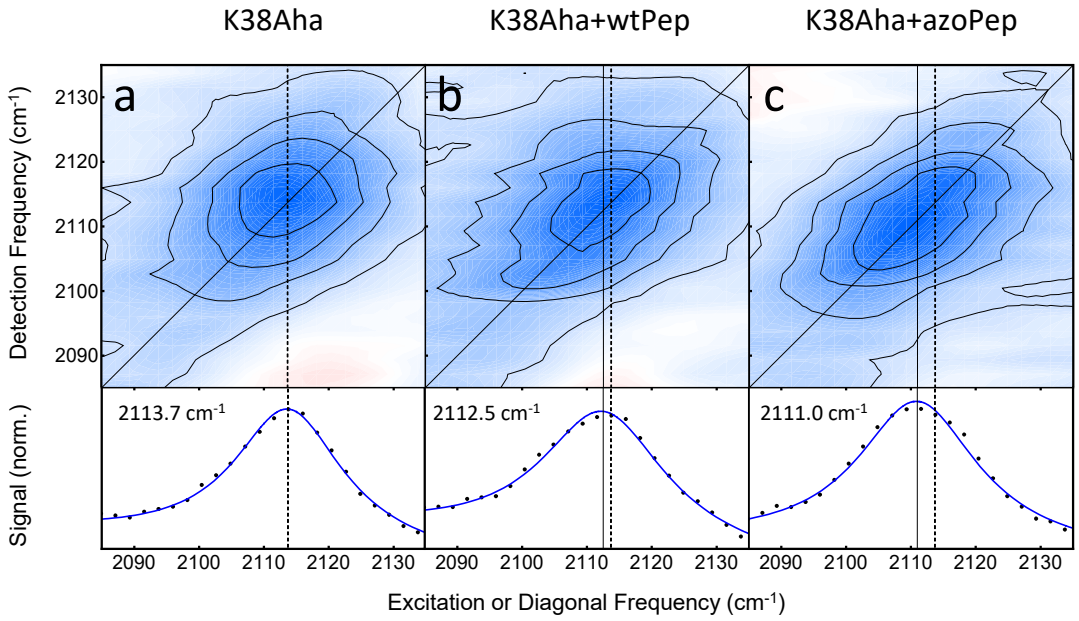

FIG. 2. Ligand binding observed with 2D IR spectroscopy. (a) 2D IR response of K38Aha, (b) K38Aha+wtPep and (c) K38Aha+azoPep. The bottom panels plot the diagonal signal together with fits used to deduce the peak position (see text for details). In panel (a) the dotted line marks the reference peak position of the Aha label without any ligand. In panels (b+c), the peak positions of the Aha label with the two different ligands are marked in addition to it as solid lines.

count the uncertainty in the phasing,[60], and by fitting the results to different models (e.g. fitting only 1D diagonal cuts as in Fig. 2 vs fitting the complete 2D line-shape or using different line-shape functions), we estimated that the statistical and systematic error in the determination of the peak-position of the Aha band is in the order of 0.5 cm^{-1}. One example of a completely different data set of K38Aha and K38Aha+wtPep is shown in Fig. S3, which has been measured with different concentration on a different day by different people. Applying the same fit function, the deduced peak frequencies are the same within 0.1 cm^{-1} as in Fig. 2, evidencing the reproducibility of the measurement. To conclude this part, for both K38Aha+wtPep and K38Aha+azoPep, we are confident that the effect is real with frequency red shifts of 1.2 ± 0.5 cm^{-1} and 2.7 ± 0.5 cm^{-1}, respectively.

B. Computational Results

Recent quantum-chemical calculations of Cho and coworkers[46,47] have shown that the spectroscopic signatures of the azido stretch mode of Aha mainly reflects the local electrostatic environment of the -N_3 reporter group. The structures shown in Fig. 1 suggest that the azido group is indeed found in different environments in each investigated case. That is, Aha is fully exposed to the solvent in K38Aha, and rarely interacts with protein atoms, while in the cases of K38Aha+wtPep and K38Aha+azoPep it is less exposed to the solvent, but interacts mostly with ligand residues. These differences are expected to be detectable in the vibrational spectra.

Indeed, using Equation (1) for calculating spectral shifts displayed in Fig. 3a, we find that the reporter group in K38Aha+wtPep and K38Aha+azoPep induces a red shift of 1-2 cm^{-1} with respect to K38Aha. To learn about the contribution of protein and solvent to the total vibrational frequency, we calculated the shifts due to protein/ligand atoms and solvent atoms independently. Considering only protein/ligand atoms, K38Aha+wtPep and K38Aha+azoPep show red shifts of 8-10 cm^{-1} and 1-3 cm^{-1} compared to K38Aha (Fig. 3b). Regarding solvent molecules only, K38Aha+wtPep and K38Aha+azoPep are blue shifted by 2-5 cm^{-1} (Fig. 3c).

To relate the vibrational shifts to changes in contact patterns, Fig. 4 compares the probability distribution of the number of azido contacts with protein/ligand and water molecules. Concerning protein/ligand contacts, K38Aha+wtPep and K38Aha+azoPep simulations exhibit 12-18 protein/ligand contacts compared to K38Aha with 9 contacts. Regarding water contacts, the azido group of K38Aha+wtPep and K38Aha+azoPep exhibit 7-8 water contacts, while K38Aha on average forms 10-12 contacts with water molecules. Hence, water contacts are replaced by ligand contacts upon binding of the peptide ligand.

To further explore the cause of red shifts of K38Aha+wtPep and K38Aha+azoPep, we calculated minimum distances between the azido group and all residues of the respective systems. We found that significant contacts only appear with ligand residues (Fig. S4), as suggested in Ref. 53. From the minimum distance

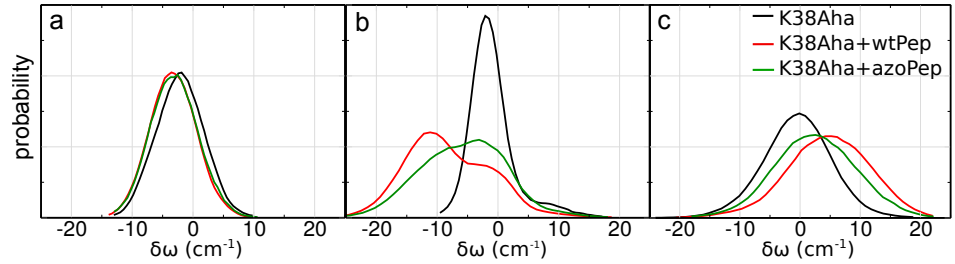

FIG. 3. Vibrational frequency shifts (relative to the vacuum value) of all simulated systems by considering (a) all atoms, (b) only protein/ligand atoms and (c) only solvent atoms.

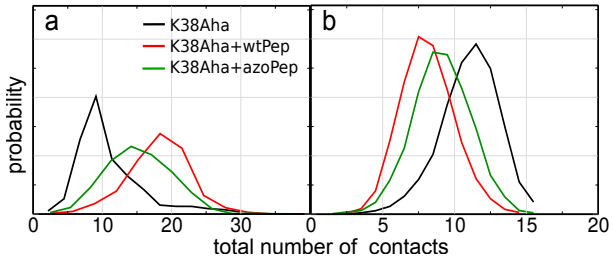

FIG. 4. Probability distribution of average number of contacts of the azido group with (a) protein/ligand and (b) solvent molecules. The black curve shows the result for K38Aha, and the red and green curves that of K38Aha+wtPep and K38Aha+azoPep, respectively.

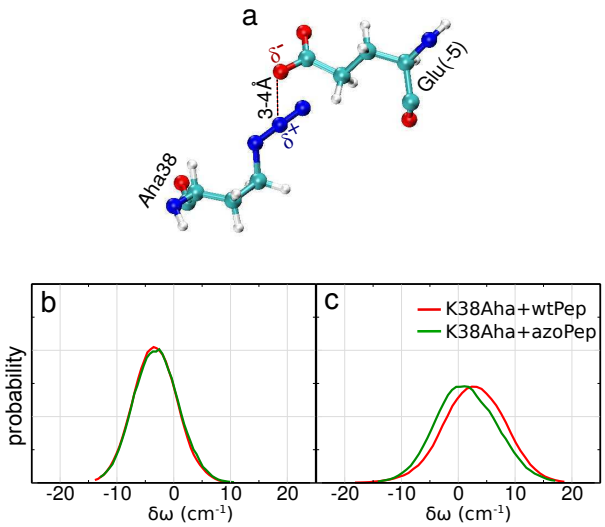

FIG. 5. (a) Polar contact between the positively charged $N^{(2)}$ of the azido group and the negatively charged side chain carboxyl oxygen of Glu(-5). (b,c) Vibrational frequency shifts of K38Aha+wtPep and K38Aha+azoPep by including (b) and excluding (c) Glu(-5).

analysis, three major contacts of Aha38 with ligand residues Glu(-5), Gln(-4) and Val(-3) were identified as potential candidates to induce red shifts. However, the distance patterns of Gln(-4) and Val(-3) do not significantly change between both protein/ligand systems, while Glu(-5) is special, as it is the only one of the three residues with significant changes in distances. That is, the middle nitrogen atom of the azido group of K38Aha+wtPep forms a consistent polar contact with the negatively charged side chain carboxyl oxygen of Glu(-5) (Figure 5a), while this contact is less stable in K38Aha+azoPep. To test if the contact with Glu(-5) is the main origin of red shifts observed in experiments and simulations, we excluded this specific residue and compared the resulting spectrum with spectra including Glu(-5) (Fig. 5b,c). Exclusion of Glu(-5) induces a blue shift of ∼4-6 cm^{-1}, with a difference of ∼2-3 cm^{-1} between K38Aha+wtPep and K38Aha+azoPep. Very likely, it is these very specific, but fluctuating contacts that give rise to the larger inhomogeneity observed experimentally upon ligand binding in the form of 2D IR line shapes that are more elongated along the diagonal (Fig. 2 b,c).

We also looked into the possible contribution of the ions in the solution to the frequency shift. Fig. S5 shows that the average distance between the azido group to the nearest ion is between 1.0 to 1.5 nm, and contacts (i.e., distances of less than 4.5 Å) almost never occur. We therefore conclude that the effect of the ions on vibrational frequency of the azido group is negligible due to the shielding by water.

IV. DISCUSSION AND CONCLUSION

We have demonstrated that it is possible to reliably measure frequency shifts of the Aha label as small as ≈1 cm^{-1} with the help of 2D IR spectroscopy, sufficient to detect rather subtle structural changes of a protein system. Furthermore, MD simulation together with pre-parameterized spectroscopic maps[47] can qualitatively reproduce the size of the spectroscopic effect. However, while the experiments reveal a bigger effect for K38Aha+azoPep than for K38Aha+wtPep, consistent with the notion that the hydrophobic azobenzene moiety might shield the Aha label more efficiently from the solvent, that effect is not reproduced by the MD sim-

ulations. On the contrary, the MD simulations suggest that interactions with very specific side chains (in this case Glu(-5)) might have a dominating effect, the exact calculation of which would require more sophisticated QM/MM simulations.[47]

It is the common notion that the frequency shift of the azido group is a measure of the amount of solvation; the stronger an azido group is solvated, the more blue is its absorption band.[15,18,28,38,45–47] Our experimental observation supports that view, with the ligands shielding the Aha label to a certain extent from water (Fig. 2). The MD results of Fig. 4b indeed show that this is the case: the number of solvent contacts is reduced once a ligand is bound to the protein. Yet, Figs. 3, 4a and 5 suggest that that this common notion needs to be re-interpreted somewhat. That is, a smaller number of water contacts is inevitably compensated by a larger number of protein contacts (Fig. 4a vs Fig. 4b), which can be polar as well; in this case in particular due to Glu(-5) (Fig. 5). These protein contacts also reveal frequency shifts due to electrostatic interactions according to Eq. (1). In fact, since the protein is more structured than the solvent, these protein contacts are more stable on average and may overcompensate the contribution of the water in terms of the frequency shift (Fig. 3). In other words, Fig. 3 reveals that all polar interactions tend to produce a frequency red shift, in contrast to the common notion, and that reduced solvation by water is overcompensated by even stronger "solvation" from the protein. It should however be noted that this interpretation is at odds with the conclusions of Ref. 38, which measured the frequency of isolated azido-groups also in very apolar solvents such as hexane, which might be assumed to be close to the situation in vacuum, but where the frequency is red shifted relative to that in water. However, in the present case, assuming the protein to be a hydrophobic bulk turns out not to be a viable approximation. Instead, especially due to the presence of Glu(-5), the protein resembles best a highly anisotropic polar "solvent" for the Aha azido group with stable charge distribution, resulting in the observed additional red shifts.

It is interesting to compare the present results to those of previous work, where we used Aha labels at various positions to detect structural changes in a PDZ2 domain that has been made photo-switchable by covalently linking a similar azo-moiety across its binding groove.[50] Only L78Aha, which sat very close to the photoswitch in the binding groove, showed an effect; in that case a change in absorption intensity rather than frequency. Also for that example we concluded that the effect is related to very specific interactions of the Aha label with the azo-photoswitch.

Previous work[15,18] has shown that Aha can be used as a reporter to determine biomolecular recognition when incorporated into the peptide ligand directly. In this study, Aha has instead been incorporated in the protein in the vicinity of the binding groove. In contrast to the ligand-incorporated reporter, we have shown by CD and ITC experiments that the presence of the Aha label neither perturbs the stability of the PDZ2 domain, nor its binding affinity for the peptide ligand, in agreement with recent NMR and X-ray experiments that came to the same conclusion for a similar molecular system.[68] The 2D IR spectra of Fig. 2 showed that Aha is indeed a sensitive probe of ligand binding, exhibiting a few wavenumbers red shift upon binding of two different peptides. MD simulations can reproduce the effect essentially quantitatively, providing an atomistic picture of the interactions of the Aha label at the protein surface. It is important to stress that the center frequency of an isolated vibrational transitions, such as that of the Aha label, can be measured with an accuracy much better than its linewidth or than the spectral resolution of the 2D IR instrument. This is the equivalent of the very idea of sub-diffraction microscopy, where the position of individual switchable fluorescing chromophores can be measured with a precision much better than the resolution of the microscope, provided that their point spread functions don't spatially overlap.[69] In conclusion, the present study demonstrates that Aha can be employed as a specific IR reporter not only for big changes of its chemical environment (e.g., protein folding/unfolding events), but also for very subtle changes of the electrostatic environment at the protein surface.

Supplementary Material: CD data (Fig. S1), ITC data (Fig. S2), an completely independently measured set of 2D IR (Fig. S3), a contact analysis of the azido group with ligand residue (Fig. S4) and the ions in solution (Fig. S5), as well as Gromacs parameters for the azo-moiety can be found in Supporting Information. This information is available free of charge on the ACS Publications website.

Acknowledgement: We thank Ben Schuler and his group for their continuous and tremendous help with the protein chemistry, Amedeo Caflisch for many insightful discussions regarding ligand binding to the PDZ2 domain, Rolf Pfister for the synthesis of the peptides, and the Functional Genomics Center Zurich, especially Serge Chesnov, for help with the mass spectrometry. The work has been supported in part by the Swiss National Science Foundation (SNF) through the NCCR MUST and Grant 200021_165789/1, as well as by the Deutsche Forschungsgemeinschaft through Grant STO 247/10-1. Computational resources were provided by the bwForCluster BinAC (RV bw16I016) and the Black Forest Grid Initiative.

(1) Pang, X.; Zhou, H.-X. Rate constants and mechanisms of protein-ligand binding, *Annu. Rev. Biophys.* **2017**, *46*, 105–130.

(2) Stelzl, U.; Worm, U.; Lalowski, M.; Haenig, C.; Brembeck, F. H.; Goehler, H.; Stroedicke, M.; Zenkner, M.; Schoenherr, A.; Koeppen, S.; et al. A human protein-protein interaction network: A resource for annotating the proteome, *Cell* **2005**, *122*, 957–968.

(3) Stanfield, R. L.; Wilson, I. A. Protein-peptide interactions, *Curr. Opin. Struct. Biol.* **1995**, *5*, 103–113.

(4) McCammon, J. A. Theory of biomolecular recognition, *Curr. Opin. Struct. Biol.* **1998**, *8*, 245–249.

(5) Huang, Z. The chemical biology of apoptosis: Exploring protein-protein interactions and the life and death of cells with small molecules, *Chem. Biol.* **2002**, *9*, 1059–1072.

(6) Arkin, M. R.; Tang, Y.; Wells, J. A. Small-molecule inhibitors of protein-protein interactions: profressing towards the reality, *Chem Biol* **2014**, *21*, 1102–1114.

(7) Babine, R. E.; Bender, S. L. Molecular recognition of protein-ligand complexes: Applications to drug design, *Chem. Rev.* **1997**, *97*, 1359–1472.

(8) Kastritis, P. L.; Bonvin, A. M. J. J. On the binding affinity of macromolecular interactions: daring to ask why proteins interact, *J. R. Soc. Interface* **2013**, *10*, 20120835.

(9) Zhao, L.; Chmielewski, J. Inhibiting protein-protein interactions using designed molecules, *Curr. Opin. Struct. Biol.* **2005**, *15*, 31–34.

(10) Piehler, J. New methodologies for measuring protein interactions in vivo and in vitro, *Curr. Opin. Struct. Biol.* **2005**, *15*, 4–14.

(11) Williams, M. A., Daviter, T., Eds. *Protein-Ligand Interactions Methods and Applications;* Springer: New York Heidelberg Dordrecht London, 2013.

(12) Greenfield, N. J. Applications of circular dichroism in protein and peptide analysis, *TrAC - Trends Anal. Chem.* **1999**, *18*, 236–244.

(13) Berggård, T.; Linse, S.; James, P. Methods for the detection and analysis of protein-protein interactions, *Proteomics* **2007**, *7*, 2833–2842.

(14) Yan, Z.; Wang, J. Specificity quantification of biomolecular recognition and its implication for drug discovery, *Sci. Rep.* **2012**, *2*, 1–7.

(15) Bloem, R.; Koziol, K.; Waldauer, S.; Buchli, B.; Walser, R.; Samatanga, B.; Jelesarov, I.; Hamm, P. Ligand binding studied by 2D IR spectroscopy using the azidohomoalanine label, *J. Phys. Chem. B* **2012**, *116*, 13705–13712.

(16) Horness, R. E.; Basom, E. J.; Thielges, M. C. Site-selective characterization of Src homology 3 domain molecular recognition with cyanophenylalanine infrared probes, *Anal. Methods* **2015**, *7*, 7234–7241.

(17) Horness, R. E.; Basom, E. J.; Mayer, J. P.; Thielges, M. C. Resolution of site-specific conformational heterogeneity in proline-rich molecular recognition by Src homology 3 gomains, *J. Am. Chem. Soc.* **2016**, *138*, 1130–1133.

(18) Johnson, P. J. M.; Koziol, K. L.; Hamm, P. Quantifying biomolecular recognition with site-specific 2D infrared probes, *J. Phys. Chem. Lett.* **2017**, *8*, 2280–2284.

(19) Basom, E. J.; Manifold, B. A.; Thielges, M. C. Conformational heterogeneity and the affinity of substrate molecular recognition by cytochrome P450cam, *Biochemistry* **2017**, *56*, 3248–3256.

(20) Waegele, M. M.; Culik, R. M.; Gai, F. Site-specific spectroscopic reporters of the local electric field, hydration, structure, and dynamics of biomolecules, *J. Phys. Chem. Lett.* **2011**, *2*, 2598–2609.

(21) Adhikary, R.; Zimmermann, J.; Dawson, P. E.; Romesberg, F. E. IR probes of protein microenvironments: utility and potential for perturbation, *ChemPhysChem* **2014**, *5*, 849–853.

(22) Kim, H.; Cho, M. Infrared probes for studying the structure and dynamics of biomolecules, *Chem. Rev.* **2013**, *113*, 5817–5847.

(23) Koziol, K. L.; Johnson, P. J. M.; Stucki-Buchli, B.; Waldauer, S. A.; Hamm, P. Fast infrared spectroscopy of protein dynamics: Advancing sensitivity and selectivity, *Curr. Opin. Struct. Biol.* **2015**, *34*, 1–6.

(24) Ma, J.; Pazos, I. M.; Zhang, W.; Culik, R. M.; Gai, F. Site-specific infrared probes of proteins, *Annu. Rev. Phys. Chem.* **2015**, *66*, 357–377.

(25) Błasiak, B.; Londergan, C. H.; Webb, L. J.; Cho, M. Vibrational probes: From small molecule solvatochromism theory and experiments to applications in complex systems, *Acc. Chem. Res.* **2017**, *50*, 968–976.

(26) Getahun, Z.; Huang, C. Y.; Wang, T.; DeLeon, B.; DeGrado, W. F.; Gai, F. Using nitrile-derivatized amino acids as infrared probes of local environment, *J. Am. Chem. Soc.* **2003**, *125*, 405–411.

(27) Koziński, M.; Garrett-Roe, S.; Hamm, P. 2D-IR Spectroscopy of the sulfhydryl band of cysteines in the hydrophobic core of proteins, *J. Phys. Chem. B* **2008**, *112*, 7645–7650.

(28) Oh, K.-I.; Lee, J.-H.; Joo, C.; Han, H.; Cho, M. Beta-azidoalanine as an IR probe: application fo amyloid Abeta(16-22) aggregation, *J. Phys. Chem.* **2008**, *112*, 10352–10357.

(29) Naraharisetty, S. R. G.; Kasyanenko, V. M.; Zimmermann, J.; Thielges, M.; Romesberg, F. E.; Rubtsov, I. V. C-D Modes of deuterated side chain of leucine as structural reporters via dual-frequency two-dimensional infrared spectroscopy, *J. Phys. Chem. B* **2009**, *113*, 4940–4946.

(30) Zimmermann, J.; Thielges, M. C.; Yu, W.; Dawson, P. E.; Romesberg, F. E. Carbon-deuterium bonds as site-specific and nonperturbative probes for time-resolved studies of protein dynamics and folding, *J. Phys. Chem. Lett.* **2011**, *2*, 412–416.

(31) Thielges, M. C.; Axup, J. Y.; Wong, D.; Lee, H. S.; Chung, J. K.; Schultz, P. G.; Fayer, M. D. Two-dimensional IR spectroscopy of protein dynamics using two vibrational labels: A site-specific genetically encoded unnatural amino acid and an active site ligand, *J. Phys. Chem. B* **2011**, *115*, 11294–11304.

(32) Thielges, M. C.; Fayer, M. D. Protein dynamics studied with ultrafast two-dimensional infrared vibrational echo spectroscopy, *Acc. Chem. Res.* **2012**, *45*, 1866–1874.

(33) Woys, A. M.; Mukherjee, S. S.; Skoff, D. R.; Moran, S. D.; Zanni, M. T. A strongly absorbing class of non-natural labels for probing protein electrostatics and sol-

vation with FTIR and 2D IR spectroscopies, *J. Phys. Chem. B* **2013**, *117*, 5009–5018.
(34) Peran, I.; Oudenhoven, T.; Woys, A. M.; Watson, M. D.; Zhang, T. O.; Carrico, I.; Zanni, M. T.; Raleigh, D. P. General strategy for the bioorthogonal incorporation of strongly absorbing, solvation-sensitive infrared probes into proteins, *J. Phys. Chem. B* **2014**, *118*, 7946–7953.
(35) King, J. T.; Arthur, E. J.; Brooks, C. L.; Kubarych, K. J. Crowding induced collective hydration of biological macromolecules over extended distances, *J. Am. Chem. Soc.* **2014**, *136*, 188–194.
(36) Bagchi, S.; Boxer, S. G.; Fayer, M. D. Ribonuclease S dynamics measured using a nitrile label with 2D IR vibrational echo spectroscopy, *J. Phys. Chem. B* **2012**, *116*, 4034–4042.
(37) Zimmermann, J.; Thielges, M. C.; Seo, Y. J.; Dawson, P. E.; Romesberg, F. E. Cyano groups as probes of protein microenvironments and dynamics, *Angew. Chem. Int. Ed.* **2011**, *50*, 8333–8337.
(38) Wolfshorndl, M. P.; Baskin, R.; Dhawan, I.; Londergan, C. H. Covalently bound azido groups are very specific water sensors, even in hydrogen-bonding environments, *J. Phys. Chem. B* **2012**, *116*, 1172–1179.
(39) Pazos, I. M.; Ghosh, A.; Tucker, M. J.; Gai, F. Ester carbonyl vibration as a sensitive probe of protein local electric field, *Angew. Chemie - Int. Ed.* **2014**, *53*, 6080–6084.
(40) van Wilderen, L. J. G. W.; Kern-Michler, D.; Müller-Werkmeister, H. M.; Bredenbeck, J. Vibrational dynamics and solvatochromism of the label SCN in various solvents and hemoglobin by time dependent IR and 2D-IR spectroscopy, *Phys. Chem. Chem. Phys.* **2014**, *16*, 19643–19653.
(41) Le Sueur, A. L.; Schaugaard, R. N.; Baik, M. H.; Thielges, M. C. Methionine ligand interaction in a blue copper protein characterized by site-selective infrared spectroscopy, *J. Am. Chem. Soc.* **2016**, *138*, 7187–7193.
(42) Basom, E. J.; Maj, M.; Cho, M.; Thielges, M. C. Site-specific characterization of cytochrome P450cam conformations by infrared spectroscopy, *Anal. Chem.* **2016**, *88*, 6598–6606.
(43) Xu, R. J.; Blasiak, B.; Cho, M.; Layfield, J. P.; Londergan, C. H. A direct, quantitative connection between molecular dynamics simulations and vibrational probe line shapes, *J. Phys. Chem. Lett.* **2018**, *9*, 2560–2567.
(44) Lee, G.; Kossowska, D.; Lim, J.; Kim, S.; Han, H.; Kwak, K.; Cho, M. Cyanamide as an infrared reporter: comparison of vibrational properties between nitriles bonded to N and C atoms, *J. Phys. Chem. B* **2018**, *122*, 4035–4044.
(45) Taskent-Sezgin, H.; Chung, J.; Banerjee, P. S.; Nagarajan, S.; Dyer, R. B.; Carrico, I.; Raleigh, D. P. Azidohomoalanine: A Conformationally Sensitive IR Probe of Protein Folding Protein Structure and Electrostatics, *Angew. Chemie - Int. Ed.* **2010**, *49*, 7473–7475.
(46) Choi, J. H.; Raleigh, D.; Cho, M. Azido homoalanine is a useful infrared Pprobe for monitoring local electrostatistics and side-chain solvation in proteins, *J. Phys. Chem. Lett.* **2011**, *2*, 2158–2162.
(47) Choi, J.-H.; Oh, K.-I.; Cho, M. Azido-derivatized compounds as IR probes of local electrostatic environment: Theoretical studies, *J. Chem. Phys.* **2008**, *129*, 174512.
(48) Kiick, K. L.; Saxon, E.; Tirrell, D. A.; Bertozzi, C. R. Incorporation of azides into recombinant proteins for chemoselective modification by the staudinger ligation, *Proc. Natl. Acad. Sci. USA* **2002**, *99*, 19.
(49) Simon, M.; Zangemeister-Wittke, U.; Plückthun, A. Facile double-functionalization of designed ankyrin repeat proteins using click and thiol chemistries, *Bioconjugate Chem.* **2012**, *23*, 279–286.
(50) Stucki-Buchli, B.; Johnson, P. J. M.; Bozovic, O.; Zanobini, C.; Koziol, K. L.; Hamm, P.; Gulzar, A.; Wolf, S.; Buchenberg, S.; Stock, G. 2D-IR spectroscopy of an AHA labelled photoswitchable PDZ2 domain, *J. Phys. Chem. A* **2017**, *121*, 9435–9445.
(51) Fuentes, E. J.; Der, C. J.; Lee, A. L. Ligand-dependent dynamics and intramolecular signaling in a PDZ Domain, *J. Mol. Biol.* **2004**, *335*, 1105–1115.
(52) Lee, H.-J.; Zheng, J. J. PDZ domains and their binding partners: structure, specificity, and modification, *Cell Commun. Signal.* **2010**, *8*, 8.
(53) Blöchliger, N.; Xu, M.; Caflisch, A. Peptide binding to a PDZ domain by electrostatic steering via nonnative salt bridges, *Biophys. J.* **2015**, *108*, 2362–2370.
(54) Kozlov, G.; Banville, D.; Gehring, K.; Ekiel, I. Solution Structure of the PDZ2 Domain from Cytosolic Human Phosphatase hPTP1E Complexed with a Peptide Reveals Contribution of the Beta 2-Beta 3 Loop to PDZ Domain-Ligand Interactions, *J. Mol. Biol.* **2002**, *320*, 813–820.
(55) Hamm, P.; Zanni, M. T. *Concepts and Methods of 2D Infrared Spectroscopy;* Cambridge University Press: Cambridge, 2011.
(56) Buchli, B.; Waldauer, S. A.; Walser, R.; Donten, M. L.; Pfister, R.; Blöchliger, N.; Steiner, S.; Caflisch, A.; Zerbe, O.; Hamm, P. Kinetic response of a photoperturbed allosteric protein, *Proc. Natl. Acad. Sci. USA* **2013**, *110*, 11725–11730.
(57) Waldauer, S. A.; Stucki-Buchli, B.; Frey, L.; Hamm, P. Effect of viscogens on the kinetic response of a photoperturbed allosteric protein, *J. Chem. Phys.* **2014**, *141*, 22D514.
(58) Kumita, J. R.; Smart, O. S.; Woolley, G. A. Photocontrol of helix content in a short peptide, *Proc. Natl. Acd. Sci. USA* **2000**, *97*, 3803–3808.
(59) Hamm, P.; Kaindl, R. A.; Stenger, J. Noise suppression in femtosecond Mid-infrared light sources, *Opt. Lett.* **2000**, *25*, 1798–1800.
(60) Johnson, P. J. M.; Koziol, K. L.; Hamm, P. Intrinsic phasing of heterodyne-detected multidimensional infrared spectra, *Opt. Express* **2017**, *25*, 2928–2938.
(61) Zhang, J.; Sapienza, P. J.; Ke, H.; Chang, A.; Hengel, S. R.; Wang, H.; Phillipsand, G. N.; Lee, A. L. Crystallographic and nuclear magnetic resonance evaluation of the impact of peptide binding to the second PDZ domain of protein tyrosine phosphatase 1E, *Biochemistry* **2010**, *49*, 9280–9291.
(62) Abraham, M. J.; Murtola, T.; Schulz, R.; Páll, S.; Smith, J. C.; Hess, B.; Lindah, E. Gromacs: High performance molecular simulations through multi-level parallelism from laptops to supercomputers, *SoftwareX* **2015**, *1-2*, 19–25.
(63) Wang, J.; Wang, W.; Kollman, P. A.; Case, D. A. Automatic atom type and bond type perception in molecular mechanical calculations, *J. Mol. Graph. Model.* **2006**, *25*, 247–260.
(64) Jakalian, A.; Bush, B. L.; Jack, D. B.; Bayly, C. I. Fast, efficient generation of high-quality atomic charges. AM1-

BCC model: I. Method, *J. Comput. Chem.* **2000**, *21*, 132–146.

(65) Jakalian, A.; Jack, D. B.; Bayly, C. I. Fast, efficient generation of high-quality atomic charges. AM1-BCC model: II. Parameterization and validation, *J. Comput. Chem.* **2002**, *23*, 1623–1641.

(66) Ernst, M.; Sittel, F.; Stock, G. Contact- and distance-based principal component analysis of protein dynamics, *J. Chem. Phys.* **2015**, *143*, 244114.

(67) Ernst, M.; Wolf, S.; Stock, G. Identification and validation of reaction coordinates describing protein functional motion: Hierarchical dynamics of T4 lysozyme, *J. Chem. Theory Comput.* **2017**, *13*, 5076–5088.

(68) Lehner, F.; Kudlinzki, D.; Richter, C.; Müller-Werkmeister, H. M.; Eberl, K. B.; Bredenbeck, J.; Schwalbe, H.; Silvers, R. Impact of azidohomoalanine incorporation on protein structure and ligand binding, *ChemBioChem* **2017**, *18*, 2340–2350.

(69) Hell, S. W. Far-field optical nanoscopy, *Science* **2007**, *316*, 1153–1158.

TOC Graphic

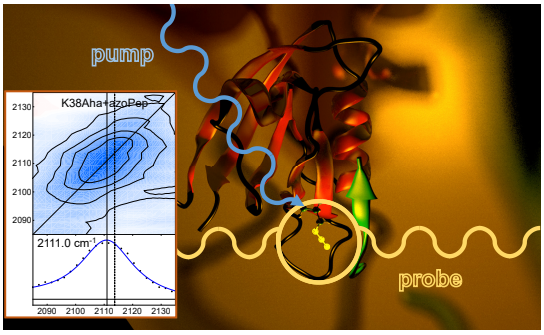
pump
K38Aha+azoPep
2130
2120
2110
2100
2090
2111.0 cm-1
2090 2100 2110 2120 2130
probe